RSC Advances

REVIEW

View Article Online
View Journal | View Issue

Cite this: *RSC Adv.*, 2022, **12**, 3505

Application of polypyrrole-based adsorbents in the removal of fluoride: a review

Ting Wang,[a] Lvji Yan,[a] Yingjie He,[a] Sikpaam Issaka Alhassan,[a] Haiyin Gang,[a] Bichao Wu,[a] Linfeng Jin*[c] and Haiying Wang *[ab]

When fluoride levels in water exceed permitted limits (>1.5 mg L^{-1}), water pollution becomes a major concern to humans. As a result, the adsorption method is the most optimal approach for treating fluorinated water due to its low cost, availability of adsorbents, pollution-free treated water, and environmental friendliness. Historically, alumina and aluminum-based adsorbents, bio-adsorbents, ion-exchange resins, calcium-based materials, carbon-based adsorbents, and polymer-based adsorbents have all been studied for the removal of fluoride ions from aqueous/wastewater. Conducting polymer-based composites have recently received a lot of attention because of their simplicity of synthesis and biocompatibility, and they could be used to treat fluoride ions. This review summarizes the physico-chemical properties, adsorption characteristics, and mechanism of various polypyrrole-based adsorbents, such as PPy/biosorbents, polypyrrole/clay mineral composites, polypyrrole/common metallic oxide composites, and polypyrrole/magnetic nanoparticles, as well as their applications in the removal of fluoride ions.

Received 20th November 2021
Accepted 19th January 2022

DOI: 10.1039/d1ra08496h

rsc.li/rsc-advances

1. Introduction

Water is a vital natural resource for the maintenance of life and is not readily accessible everywhere.[1] With rapid urbanization and exponential industrial growth, groundwater contamination has increased substantially thus far. So far, 2.0 billion people lack safe drinking water and this figure is anticipated to reach 4.6 billion by 2080.[1–3] Fluoride is a double-edged sword that acts as a necessary micronutrient and is capable of preventing dental caries and enhancing mineralization of hard tissues.[1,4,5] However, high fluoride levels in drinking water supplies lead to serious safety concerns and may induce dental and skeletal fluorosis, which are viewed as major health hazards in most developing nations.[6–8] Drinking water guidelines prescribe an acceptable fluoride content of 1.0 mg L^{-1}, whereas the World Health Organization (WHO) defines an acceptable fluoride concentration of 1.5 mg L^{-1} in drinkable waters.[9] There is evidence that quantities of fluoride in groundwater over 30 mg g^{-1} are frequent in more than 30 countries globally, mainly in Asia, America, and Africa.[10,11] During the recent past, different strategies have been explored to remove fluoride ions from water which include adsorption,[12–16] ion exchange,[17,18] membrane separation,[19] electrolytic defluoridation,[20] coagulation–precipitation[21] and so on. Among these methods, adsorption is still one of the most widely used methods for defluoridation of water due to its low cost, feasibility, and ability to remove fluoride ions.[22–26] Furthermore, the adsorption technique has a favorable fluoride removal ability in addition to the advantages already described, and the design and operation of the device are easy. Importantly, adsorbents are readily accessible with unique environmental friendliness and potential for re-use. Examples of commonly used adsorbents are modified alumina, metal oxides, carbon-based materials, biomass, metal–organic frameworks, and polymer-based adsorbents.[27,28] However, these materials have several difficulties, such as complicated synthesis processes, environmental instability, secondary contamination, and prohibitive raw material costs.[3,29,30] Polypyrrole, a conducting polymer has been picked as the principal object of concern owing to its easy synthesis process, as well as its ability to easily scavenge fluoride ions.[31] Currently, there is no evaluation of the fluoride removal performance of polypyrrole and polypyrrole-based composites thus warranting investigation.

Fluoride removal from water by polypyrrole and polypyrrole-based composites is largely based on ion exchange and electrostatic interaction, the rationale for the ion exchange of polypyrrole is that charge balance or electroneutrality of the polymer matrix is maintained by incorporation of exchangeable counter anions from the reaction solution during chemical polymerization of pyrrole.[32,33] Ppy can be easily manufactured by chemical or electrochemical polymerization processes with charges in the polymer, which are part of the nitrogen atoms in

[a]*School of Metallurgy and Environment, Central South University, Changsha, China. E-mail: haiyw25@yahoo.com*

[b]*Chinese National Engineering Research Center for Control & Treatment of Heavy Metal Pollution, Changsha, China*

[c]*School of Material Science and Engineering, Central South University, Changsha, China. E-mail: jlfcsu@163.com*

polypyrrole positively charged. The occurrence of positively charged nitrogen atoms in polymer can cause electrostatic interaction with anions.[32,34] Current literature on polypyrrole and polypyrrole composites for fluoride removal can be put into the following groups: (i) polypyrrole, (ii) polypyrrole bio-adsorbents, (iii) polypyrrole/clay minerals composites, and (iv) polypyrrole/inorganic nanocomposites.

The preparation of polypyrrole is mainly through *in situ* oxidation polymerization technique of which ion exchange and electrostatic interaction are the key processes of fluorine removal. However, the adsorption capacity of most polypyrrole does not often exceed 6.37 mg g^{-1},[32] a limitation that needs to be looked at. Biomass-based materials have gained substantial research attention due to their huge surface areas, availability, and low cost. The incorporation of bio-materials into polypyrrole has been reported as a key strategy for enhancing the adsorption capacity.[35] Moreover, the addition of clay minerals into polypyrrole has been noted to improve the surface area and reduce the aggregation of PPy particles of π–π stacking.[36] The too little surface area of organic polymers can be improved through the addition of nanoparticles with a huge surface area, which may open a new window to increasing the adsorption capacity of polypyrrole. Consequently, other studies[37–39] have reported that the fabrication of hybrid polypyrrole nanocomposite can substantially increase the adsorption capacity to about 31.93 mg g^{-1} at near-neutral pH.

Therefore, this study examines all the successes and shortfalls of recent works on fluoride adsorption utilizing polypyrrole and polypyrrole-based composites (Table 1). Extensive literature has been reviewed on the synthesis methods, different modifications of polypyrrole and the mechanism of sorption have been well explored. Additionally, the influence of water chemistry parameters such pH, temperature, and inorganic anions on the performance of polypyrrole and polypyrrole-base composites have been examined.

2. Polypyrrole and polypyrrole-based composites

2.1 Polypyrrole

A five-membered ring made up of one nitrogen atom and four carbon atoms is known as pyrrole monomer. Chemical synthesis and electrochemical synthesis are both used to polymerize pyrrole monomer, with chemical oxidation being the most prevalent. Due to its redox characteristics, high conductivity, strong environmental stability, and ease of processability, PPy has been intensively investigated for a variety of possible applications.[52] Ferric salt, potassium permanganate, persulfate, and other oxidants are often used in chemical oxidation polymerization. Because of the high mobility of these ions across the PPy matrix, anions doped into ppy as tiny size dopants, such as Cl^-, ClO_4^-, and NO_3^-, display anion exchanging behavior. Many researchers have described the synthesis of polypyrrole by chemical oxidative polymerization in a variety of substrates and recipes, and the ion adsorption effectiveness of PPy is heavily influenced by the *in situ* synthesis circumstances. Various attempts have been made in a variety of ways to remove fluoride ions from contaminated water using polypyrrole adsorption, however, fluoride removal effectiveness by polypyrrole still has to be improved. More research into the effects of other anionic dopants on fluoride removal, such as Cl^-, ClO_4^-, NO_3^-, and SO_4^{2-}, should be done in the future. Because of its small size and high mobility, PPy intercalated with Cl^- ion has a greater ion exchange capacity than other ions.[32,40,52,53] Moreover, due to the presence of nitrogen atoms in the polymer chains, PPy has also shown vivid foreground in the area of defluorination. The use of polypyrrole conducting polymers to remove fluoride has been the subject of extensive investigation. Its adsorption effectiveness mostly depends heavily on the circumstances used to generate it.[27] Several chemical oxidative polymerization of pyrrole has been investigated with different dopants under varied conditions. The oxidation of pyrrole monomers into radical cations in the presence of $FeCl_3$ initiates the *in situ* polymerization step (Fig. 1(a)).[52] The water-insoluble polypyrrole is generated while the polymerization process continues. The Cl^- anion intercalation can act as an anion exchanger with anions found in wastewater (Fig. 1(b)). One of the experiments used $FeCl_3$ as an oxidant to make PPy by chemical oxidative polymerization. The pH of the solution, the dose of the adsorbent, the starting concentration, and the contact period were all studied in this investigation. PPyCl has a fluoride ion adsorption capability of 6.37 mg g^{-1}. Therefore, due to the lower size of F^- ions, they may be removed *via* ion exchange with chloride ions onto the surface of PPyCl.[32]

Moreover, both $FeCl_3 \cdot 6H_2O$ and $Fe_2(SO_4)_3$ were employed as an oxidant in one of the investigations to produce PPy–Cl and PPy–SO_4 for fluoride removal. The kinetics of PPy–Cl was rapid with higher adsorption capacity (13.98 mg g^{-1}), which was about 4 times that of the PPy–SO_4 (3.08 mg g^{-1}) and PPy–SO_4 + Cl (3.17 mg g^{-1}). The mechanism of removal was ion exchange between F^- and Cl^- or SO_4^{2-} and Cl^- was more favorable than SO_4^{2-}. The EDX data (Fig. 2 and Table 2) revealed that following fluoride adsorption, the peak intensity of the Cl and S elements decreases (Fig. 2(a) and (b)). However, in the adsorption of F^- by PPy–SO_4 + Cl, the concentration of Cl was reduced before that of S (Fig. 2(c)). These findings imply that the ion exchange process between F and Cl is higher than F and SO_4^{2-} and the addition of SO_4^{2-} to Cl causes a significant reduction in Cl hence decreasing its ion exchange potency.[40]

2.2 Polypyrrole bio-adsorbents

Because biomass material is eco-friendly, biocompatible, low cost, and renewable, adsorption of fluorides utilizing different PPy-based bio adsorbents is a highly promising technique. Biomass materials, such as charcoal,[54] pomelo peel,[55] and chitosan,[56] are widely recognized as effective adsorbents for fluoride removal. Polypyrrole/chitosan, polypyrrole-grafted peanut shell biological carbon, and polypyrrole-modified pomelo peel biochar are currently being developed. Due to the large specific surface area of biomaterials, their incorporation into polypyrrole may reduce or even prevent particle aggregation. This can initiate or strengthen the already existing electrostatic

Table 1 Comparative evaluation of polypyrrole and polypyrrole-based adsorbents for de-fluorination

Material categories	Adsorbent	Surface area $m^2\ g^{-1}$	Conc. mg L^{-1}	Dosage (g L^{-1})	pH range	Temp. (°C)	Contact time (min)	Maximum adsorption (mg g^{-1})	Mechanism	Ref.
PPy	PPy	—	2–10	0.5–4	3–10	30–50	5–30	6.37	Ion-exchange	32
	PPy–Cl	—	10	2	5	15–35	0–120	13.98	Ion-exchange, electrostatic attraction	40
PPy bio-adsorbents	PPy/Ch	—	2–10	0.5–4	3–9	30–50	5–30	6.7	Ion-exchange	41
	PPy-grafted BC(peanut shell)	37.24	4.6–87.8	2–20	2–10	25 ± 2	1440	17.15	Ion-exchange, electrostatic attraction, mesoporous diffusion	6
	PPy-grafted BC(pomelo peel)	—	10–300	1–5	2.8–10	25 ± 2	1440	18.52	Ion-exchange, electrostatic attraction	35
PPy/clay minerals composites	PPy-MMT	—	2–10	0.5–3	—	30–50	5–30	5.1	Ion-exchange, physical adsorption	37
	PPyCl/ATP	—	5–21	0.1–0.35	1–12	25–55	30–150	2.67	Ion exchange	42
PPy/common metallic oxide composites	PPy–AlO	—	2–10	0.5–4	3–9	30–50	5–30	8	Ion-exchange, coordination interaction	43
	PPy/HSnO	65.758	5–20	0.1–4	3.5–8.5	25–55	1440	28.99	Ion-exchange, electrostatic interaction	44
	$HTiO_2$@PPy	98.17	10	0.2–4	6.5	25	5–30	31.93	Ion-exchange, electrostatic interaction	45
	PPy/TiO_2	95.71	20	0.5–3	1–13	25–45	0–180	33.178	Ion-exchange, electrostatic interaction, chelation	46
	Zr–PZI	308.76	50–500	0.2–2	2–9	30–50	40	183.5	Ion-exchange, electrostatic interaction, ligand exchange	47
	MgO_2/Ppy	—	6–14	0.1–0.6($\times 10^{-3}$)	3–11	30	10–60	4.328	Ion-exchange, electrostatic interaction	48
PPy/magnetic nanoparticles	PPy/Fe_3O_4	1206.53	10–60	0.5–4	2–10	25–45	20	22.3	Ion-exchange	49
	CZFO/PPy	68.4	30–70	0.5–2	1–13	25	10	27.5	—	50
	Ni/PPy	47.304	5–40	0.1–4	3–11	25	180	67.71	—	51

attraction and/or ion exchange of polypyrrole to fluoride ions thus substantially boosting the adsorption capacity of fluoride ions. Except for cellulose, chitosan (CS) is the most abundant biological resource with cheap cost, chemical inertness, biocompatibility, biodegradability, and high mechanical strength.[57,58] Because of its high amount of active amino ($-NH_2$)

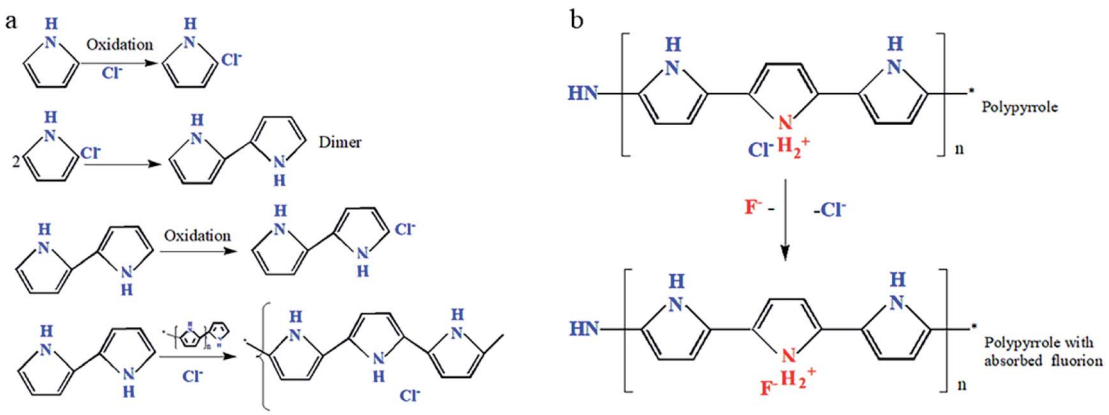

Fig. 1 Scheme of formation of polypyrrole in presence of $FeCl_3$ (a) and adsorption of fluoride ions on the surface of nitrogen functional groups in PPy (b).[52]

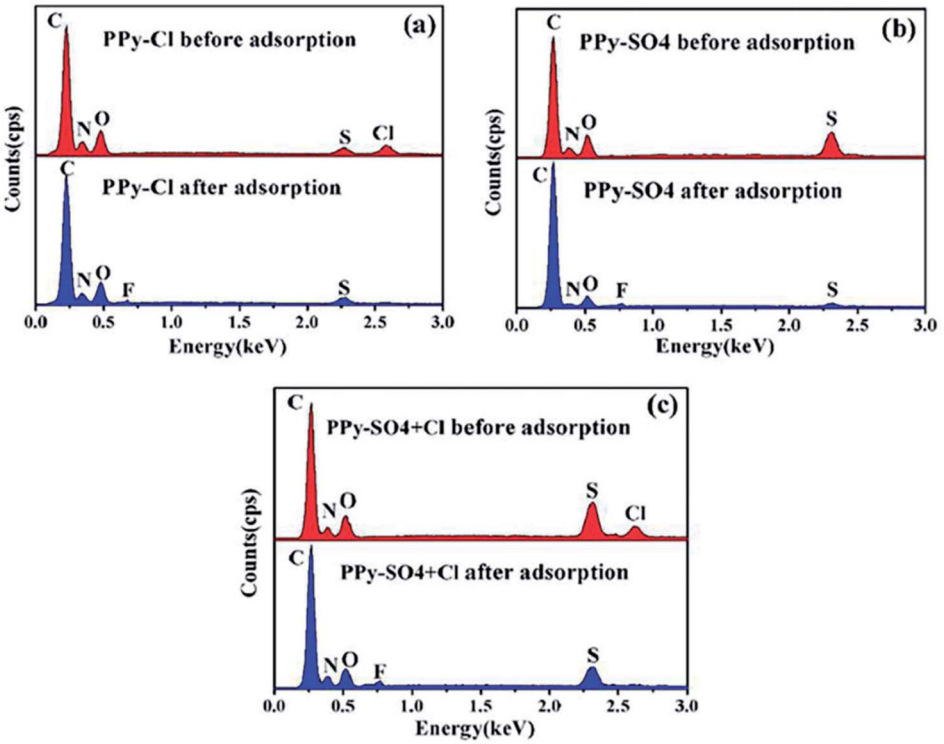

Fig. 2 The element variation of PPy samples before and after fluoride adsorption: a PPy–Cl; b PPy–SO_4; c PPy–SO_4 + Cl.[40]

Table 2 The element contents of PPy samples before and after fluoride adsorption by EDX[40]

Samples	F (A%)	S (A%)	Cl (A%)
PPy–Cl before adsorption	—	—	3.31
PPy–Cl after adsorption	1.29	—	1.28
PPy–SO_4 before adsorption	—	3.05	—
PPy–SO_4 after adsorption	0.51	0.98	—
PPy–SO_4 + Cl before adsorption	—	3.7	1.05
PPy–SO_4 + Cl after adsorption	0.85	2.19	0.12

and hydroxyl (–OH) groups, CS has an exceptional ability to successfully remove dye, metal ions, and anions from wastewater.[59] Fluoride ions were removed from water solutions using polypyrrole/chitosan (PPy/Ch) as an eco-friendly adsorbent.[41] The effects of starting sorbate concentration, adsorbent dosage, pH, co-ions, agitation period, and temperature on fluoride ion removal efficiency were comprehensively investigated in this study. The results revealed that when the initial sorbate concentration increased, the number of fluoride ions adsorbed per unit mass of the adsorbent increased, owing to the availability of a greater number of active sites per unit mass of the adsorbent. The absorption of fluoride ions rises with increasing temperature, showing that the process is endothermic, and the fluoride was completely removed in 10 minutes. The impact of adsorbent dosage was also investigated, with results showing that the amount of fluoride ion eliminated increased as the adsorbent dose was reduced, and subsequent tests were carried out to determine the ideal dose of 25 mg of adsorbent per 50 mL of fluoride ion solution. Adsorption at the solute/solid interface is usually influenced by pH.[41] As a result, the adsorption of fluoride ions at pH values ranging from 3 to 9 was investigated. The number of fluoride ions adsorbed (Q_e) for PPy/Ch fell from 5.74 to 3.3 mg g^{-1} as pH was increased. More N-atoms in component polymers are protonated at acidic pH ranges, and this positively charged nitrogen moiety electrostatically ensnares fluoride ions.[32,60] The results showed that defluoridation capability was excellent throughout a wide pH range, particularly around neutral pH. The findings revealed that common co-ions such as Cl, SO_4^{2-}, and HCO_3^- have no discernible influence on fluoride elimination.

Peanut shell is a high-volume, low-density agricultural waste. Peanut shells have been used as an adsorbent to increase their value and availability in recent years.[61] According to Li *et al.*,[6] the PPy-grafted BC (PPy/BC) composite has a lot of promise for fluoride removal from an aqueous solution. A PPy/BC dosage of 10 g L^{-1} at a contact period of 6 hours achieved a maximum adsorption capacity of 17.15 mg g^{-1}. Importantly, this compound has good characteristics from pH 2.0 to 10.0 and demonstrated significant fluoride selectivity in the presence of other co-existing anions. Wang *et al.*[35] employed another biochar made from slow pyrolysis of pomelo peel as a foundation material to create a new low-cost PPy-modified BC adsorbent with a positive charge at pH 8.6, a wide pH range of 2.8–10, and a high adsorption capacity. At 25 °C, the highest adsorption capacity was 18.52 mg g^{-1}. At pH 5.0, 2.5 g L^{-1} of BP-0.1 effectively reduced F from 10.0 to 1.4 mg L^{-1}, according to groundwater research. Ion exchange and electrostatic attraction

were shown to be the predominant adsorption mechanisms throughout the characterization process.

Chemical polymerization may be used to generate polypyrrole bio-adsorbents with high defluoridation capabilities and low environmental impact, as well as a sufficient thickness and uniformity of film, making it a preferable approach for PPy deposition on a substrate. Low fluoride adsorption capacity, sluggish adsorption rate, and extended adsorption time are still issues. To simplify the synthesis process and lower large-scale expenses, future research should investigate using readily available biomass materials that are both effective and cost-effective. Before oxidative polymerization with pyrrole, chemical reagents including cations, acids, and bases can be used to change biomass materials to provide them a greater surface area with good pore size and volume distribution, hence enhancing the fluoride removal capability of polypyrrole bio-adsorbents.

2.3 Polypyrrole/clay minerals composites

Composite materials derived from polymers and inorganic materials can achieve many synergistic properties that are difficult to achieve from individual components.[18] Because of their intercalation property, small particle size, and abundant resources, clay minerals have been used in the field of polymer composites to remove toxic metal ions, organic pollutants, and fluoride ions.[62–66]

For many years, montmorillonite clay (MMT) and Attapulgite (ATP) have been used in a variety of applications, and they are abundant in nature.[67,68] Because of its important biological activity, montmorillonite clay has been used to treat tropical diseases. The adsorption capacity of modified montmorillonite with expandable layered structure and large surface area is exceptional.[69] The chemical oxidative polymerization of pyrrole with ferric chloride as an oxidant was used to make conducting polymer/montmorillonite (PPy–MMT) composites.[37] During the synthesis, pyrrole (2.1 mL) and montmorillonite (2 g) were added to 50 mL of methyl alcohol and stirred for 10–15 minutes with a magnetic stirrer, followed by the addition of ferric chloride (7.18 g) at about 0–5 °C under continuous stirring for 16 hours. Finally, the product was filtered and thoroughly washed with methyl alcohol before being dried in a 60 °C oven for 24 hours. At 30 °C, the PPy–MMT composite showed significant potential for the removal of fluoride ions, with 5.1 mg g^{-1} compared to 2.66 mg g^{-1} for the polymers alone, indicating that the higher temperature facilitates fluoride removal. The ion-exchange mechanism is used by these chloride ion-doped polymers to remove fluoride ions from aqueous solution, and the change in elements can be seen in the EDAX patterns of the polymer (Fig. 3) before and after fluoride ion adsorption. The physical adsorption mechanism is used by montmorillonite to adsorb fluoride ions. As a result, the PPy–MMT composite uses a combination of ion exchange and physical adsorption mechanisms to remove fluoride ions from an aqueous solution.

Attapulgite (ATP) is a fibrillar-structured crystalline hydrated magnesium aluminum silicate mineral.[70] Adsorbents with exchangeable cations and reactive –OH groups on their surface, such as ATP and activated ATP, have been widely used to remove heavy metal ions and organic pollutants.[71] Organic modified ATP with small molecules or polymers has recently been studied extensively for the removal of harmful ions in groundwater. Chen *et al.*[42] used *in situ* polymerization with ferric chloride as an oxidant and 1 g ATP and pyrrole (1 mL) added to the solution to make PPyCl/ATP composites, which they used as an adsorbent to remove fluoride ions from aqueous solutions. The effects of external factors such as initial F^- concentration, solution pH, adsorbent dosage, and contact time on composite adsorption efficiency were investigated. At a sorbent dose of 0.18 g, the adsorption efficiency was 74.71%, and the optimum sorption conditions were 1.5 hours of contact time, 12 mg L^{-1} initial concentration, and an optimal pH of 5.1.

Clay minerals have a small particle size, intercalation property, abundant reactive groups, and are extensively abundant. Consequently, composites of polypyrrole and clay minerals have superior fluoride removal capacity and several synergistic properties that are difficult to obtain from individual components. However, their fluoride removal capacity still needs to be improved. Before oxidative polymerization with pyrrole, activating clay minerals by heat treatment or other chemical activation to increase their active functional groups and the specific surface is a worthwhile choice. More clay minerals could be used in conjunction with pyrrole, and clay minerals should be modified with elements like rare-earth metals, which have highly electropositive properties and a higher affinity for fluoride, ensuring a higher adsorption rate.

2.4 Polypyrrole/inorganic nanocomposites

Conducting polymer/inorganic hybrid composites combine the advantages of both elements and are gaining popularity. Because of strong π–π* interactions between PPy main chains, they exhibit unique hybrid thermal, physical, chemical, and mechanical characteristics that preclude polypyrrole aggregation. As pure polymers and inorganic hosts, polymer composites with larger surface area and shorter diffusion route lengths have good adsorption capabilities.[43,44,72]

2.4.1 Polypyrrole/common metallic oxide composites. PPy/metallic oxide nanocomposites in various forms, sizes, and shapes have recently been employed for the adsorption of fluoride ions from wastewater or an aqueous solution.[43–46,48–51] For the elimination of fluoride ions, polypyrrole/alumina (PPy–AlO) composites,[43] polypyrrole/hydrous tin oxide nanocomposites (PPy/HSnO),[44] hydrous titanium oxide@polypyrrole ($HTiO_2$@PPy),[45] polypyrrole/TiO_2,[46] MgO_2/Ppy hybrid nanocomposite,[48] and zirconium(IV) have been studied. For fluoride removal, polypyrrole/alumina (PPy–AlO) composites were made by *in situ* polymerization of pyrrole monomer. The results revealed that the adsorbent's adsorption capacity is greater than that of the individual components, with a maximum adsorption capacity of 8 mg g^{-1}.[43] Polypyrrole/hydrous tin oxide nanocomposites (PPy/HSnO) were made by encapsulating HSnO in PPy by *in situ* polymerization to remove fluoride. The adsorbent's BET surface area and pHpzc were calculated to be 65.758

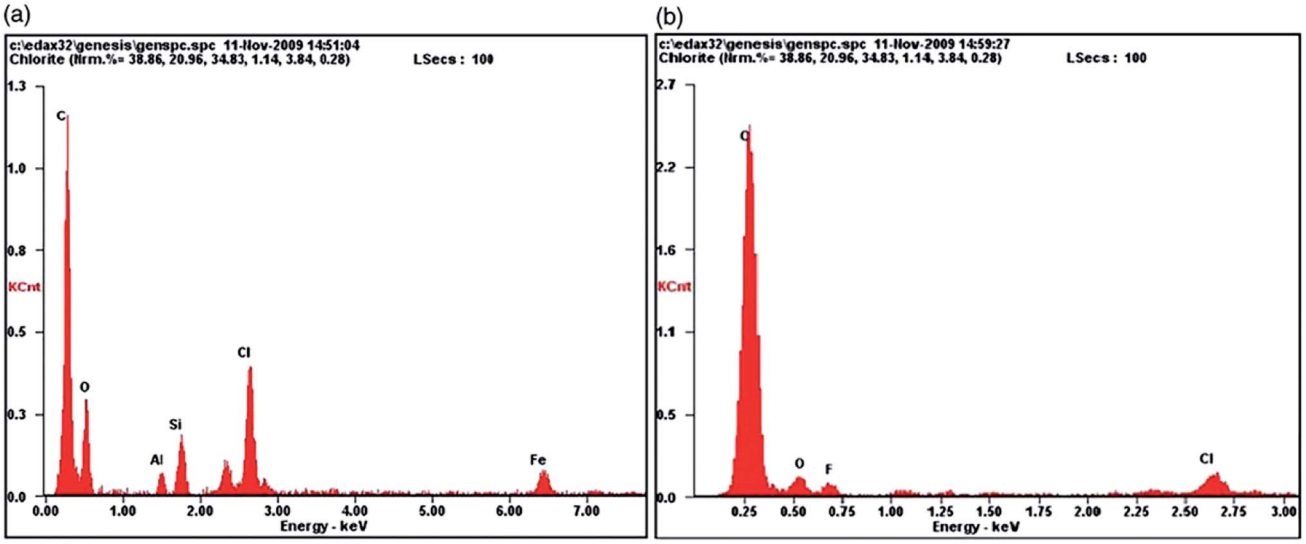

Fig. 3 EDAX patterns of PPy–MMT composite (a) before (b) after the adsorption with fluoride ions.[37]

$m^2\ g^{-1}$ and 7.6, respectively, which are favorable for defluorination. At pH 6.5, the monolayer adsorption capacity was 26.16–28.99 mg g^{-1}. The potential of an electrical interaction between F^- ion in aqueous solution and PPy/HSnO at a pH lower than pHpzc may be explained in two ways: (1) electrostatic interaction in aqueous solution between the positively charged core (nitrogen) of PPy and the negatively charged F^- ion (2). In aqueous solution, the positively charged surface hydroxyl group of HSnO usually in acidic medium, interacts with the negatively charged F^- ion *via* electrostatic contact. Furthermore, an ion-exchange reaction mechanism may be characterized when the pH of the aqueous medium remains largely within the range of pHpzc, F^- ion adsorption onto the electrically neutral surface of the adsorbent occurs: (1) ion exchange process in aqueous solution between doped Cl^- ions of the PPy chain and negatively charged F^- ions, and (2) ion exchange reaction in aqueous solution between loosely bound surface hydroxyl groups of HSnO.[44]

$HTiO_2$@PPy was made by suspending $HTiO_2$ nanoparticles in aqueous solution after a simple *in situ* chemical oxidative polymerization of pyrrole monomer. The adsorbent had a larger BET surface area of 98.17 $m^2\ g^{-1}$ and a higher pHpzc of 8.4 value. At pH 6.5 and 25 °C, the highest adsorption was 31.93 mg g^{-1}, and the adsorbent had outstanding F^- sorption selectivity with three-cycle regeneration performance. Electrostatic interactions and ion-exchange are two putative underlying mechanisms. *In situ* chemical oxidative polymerization was used by Chen *et al.* to make a PPy/TiO_2 composite. The formation of the PPy homopolymer and the presence of glycine in the PPy matrix have been confirmed by XRD and XPS analysis, respectively (Fig. 4). The peaks in the XRD patterns indicate no discernible difference between TiO_2 and PPy/TiO_2, suggesting that the amorphous polymer simply covers the surface of TiO_2 rather than integrating into the TiO_2 layers. At 25 degrees Celsius, the maximum adsorption was 33.178 mg g^{-1}. Moreover, the adsorbent was able to reduce fluoride content in the drinking water from 11.678 mg L^{-1} to 1.5 mg L^{-1} within 30 minutes at pH 7 with 6 cycles of regeneration without losing its adsorption potency. The adsorption mechanism was primarily ion exchange and electrostatic attraction.[46] A Zr(IV)—doped polypyrrole/zirconium(IV) iodate composite was fabricated to remove fluoride ions, and the maximum amount of adsorption was found to be 183.5 mg g^{-1} at pH 6.8.[47]. Unlike others, the synthetic approach is unique, a white gelatinous precipitate of zirconium(IV) iodate (ZI) and a polypyrrloe gel were prepared separately, then the gel of polypyrrloe was added to the white gelatinous precipitate of zirconium(IV) iodate and the pH of the mixture was adjusted to 1, then the mixture was stirred on a magnetic stirrer at 30 °C for 24 hours and dried in a 50 °C oven. Finally, PZI was treated for 2 hours at room temperature with steady stirring with 0.1 M zirconium oxychloride, resulting in Zr(IV) being adsorbed on the PZI by ion exchange. Fig. 5 illustrates the synthesis of Zr-PZI. At neutral pH, ion-exchange is the primary process on the adsorbent surface, where Cl ions are exchanged with fluoride ions. Because both F^- and OH^- are isoelectronic and have a similar ionic radius, the weakly attached surface hydroxyl group of zirconium(IV) iodate was replaced by the fluoride ion. Zr(IV) species, such as $ZrOOH^+$, adsorb on the adsorbent during doping. As a result, fluoride ions attack ZrOOH, causing –OH to be displaced from ZrOOH, allowing for surface adsorption. Ultimately, excellent fluoride removal performance can be attributed to a large number of sites accessible for F binding.

2.4.2 Polypyrrole/magnetic nanoparticles. After defluorination, the topic of separating polypyrrole-based composites from liquid bulk has gotten a lot of attention. Separation techniques such as filtration and centrifugation are widely employed. The magnetic characteristics of the composite of polypyrrole and magnetic nanoparticles allow them to be successfully removed from the system by an external magnetic field after adsorption, boosting separation efficiency, simplifying the separation process, and avoiding

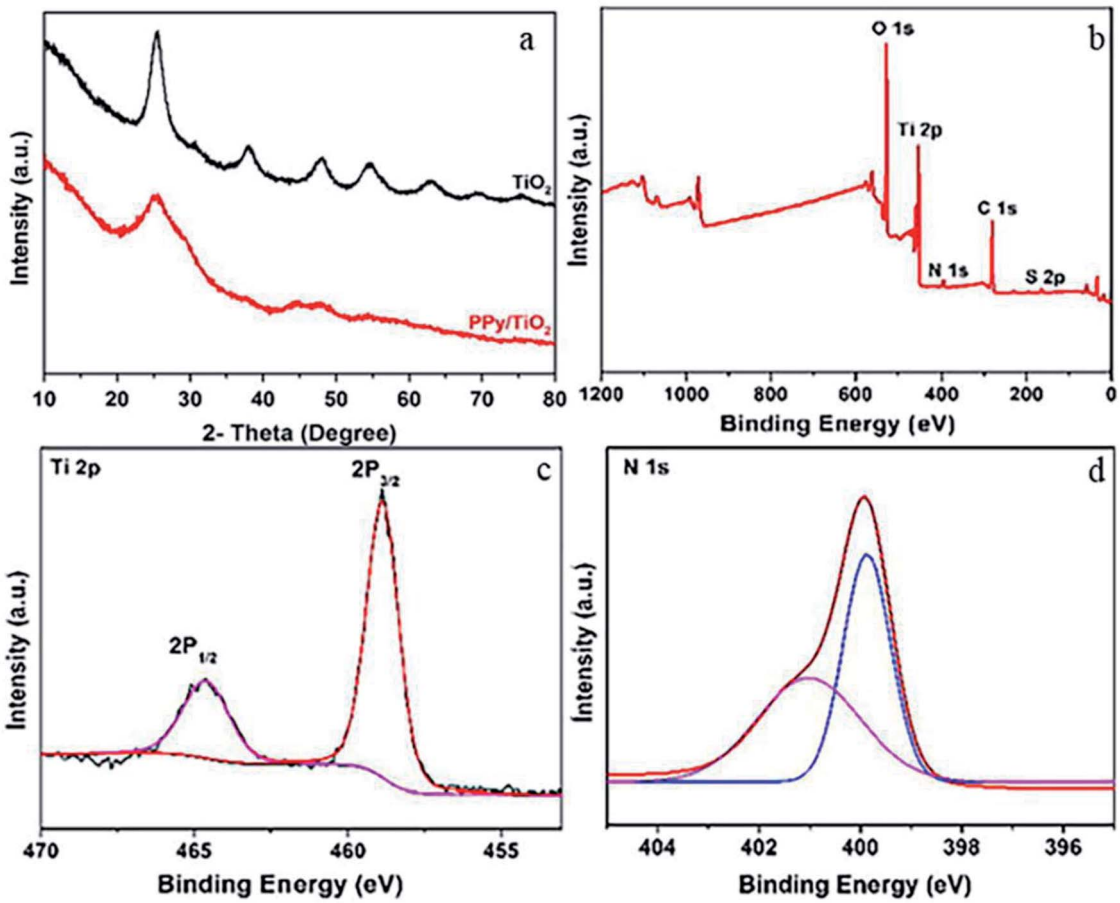

Fig. 4 XRD patterns of the as-prepared TiO_2 and PPy/TiO_2 composite (a) and XPS full scale and Ti 2p, N 1s core level spectra of the PPy/TiO_2 composite (b–d).[46]

secondary contamination. For fluoride adsorption, polypyrrole/Fe_3O_4 magnetic nanocomposites, magnetic nickel/polypyrrole (Ni/PPy) nanostructures, and $Co_{0.5}Zn_{0.5}Fe_2O_4$/polypyrrole (CZFO/PPy) nanocomposites have been developed.

In situ polymerization of pyrrole monomer employing $FeCl_3$ oxidant in aqueous solution with Fe_3O_4 nanoparticles for fluoride ion removal was used to make Fe_3O_4 coated PPy magnetic nanocomposite.[49,73] The presence of PPy polymeric moieties in the nanocomposite is confirmed by the ATR-FTIR spectra (Fig. 6(c)). After adsorption with fluoride ions, all peak locations in the PPy/Fe_3O_4 nanocomposites are pushed towards higher values, showing that the more electronegative fluoride ions adsorb on the surface of the PPy/Fe_3O_4 nanocomposites by replacing doped chloride ions. The surface area was about 1206.53 $m^2\ g^{-1}$.[49] Fig. 6(a and b) shows scanning electron micrographs of (a) Fe_3O_4, and (b) PPy/Fe_3O_4 nanocomposites before and after fluoride adsorption. The production of spherical particles and aggregates with an average diameter of 10 nm can be seen in the SEM image of Fe_3O_4 (Fig. 6(a)). PPy/Fe_3O_4 nanocomposite, on the other hand, produced almost spherical particles with greater diameters than Fe_3O_4 nanoparticles (Fig. 6(b)).[49] The production of polymer-based nanocomposites resulted from the encapsulation of nano dimensional Fe_3O_4 particle suspensions in the aqueous medium by precipitating polymeric moieties, as shown by the aforementioned features. The XRD pattern did not change significantly before and after fluoride treatment (Fig. 6(d)), indicating that ion exchange is the primary mechanism for fluoride removal in PPy/Fe_3O_4 nanocomposites.[49] In general, the nanocomposite is more effective at pH levels that are close to neutral or alkaline. With a pH of 6.5 to 8.5, the nanocomposite performs best in defluoridation of drinking water.

An *in situ* chemical oxidative polymerization of pyrrole monomers in the presence of $FeCl_3$ oxidant in an aqueous solution of Ni nanoflowers was used to create magnetic nickel/polypyrrole (Ni/PPy) nanostructures in another investigation.[51] In the real groundwater of Assam, India, the maximum amount of Ni/PPy adsorption for As(III) and F^- were 2.64 and 67.71 mg g^{-1}, respectively, and it exhibited excellent adsorption efficiency.[51] The number of spherical particles increases as the number of Py increases in the FESEM picture of Ni/PPy composites. The agglomeration of spherical particles almost eliminated the flower-like nickel when the Ni/Py weight ratio was 1 : 2 (Fig. 7(I)). In Fig. 7(II) and Table 3, the ferromagnetic behavior of Ni/PPy is shown, and the value of Ms decreases with

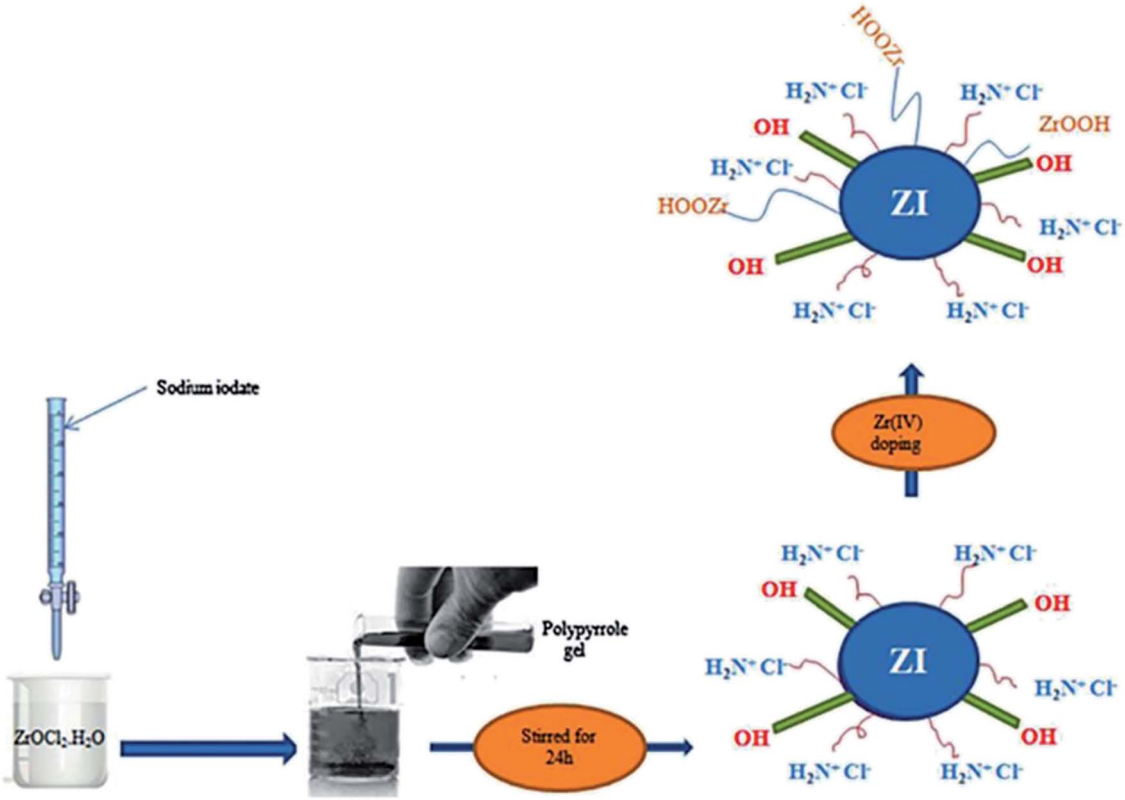

Fig. 5 Synthesis of Zr(IV)–polypyrrole zirconium(IV) iodateb.[47]

increasing PPy concentration.[51] After eluting with HCl/NaOH, its separation is enhanced and made more easily.

Microfluidic reactors were used to create highly dispersed $Co_{0.5}Zn_{0.5}Fe_2O_4$/polypyrrole (CZFO/PPy) nanocomposites with improved electromagnetic characteristics and a wide surface area. The composites' highest Ms value was 21 emu g^{-1}, which is sufficient for magnetic separation and fluoride ion adsorption control.[50] Differences in the dispersibility of nanocomposites produced in batch reactors *vs.* those synthesized in microfluidic reactors can be attributed to differences in reaction flow patterns.

In a batch reactor, turbulent flow arises because reactant mixes can flow in any direction without colliding with the walls. In a microfluidic reactor, laminar flow occurs when the reactant fluid is forced to flow in one direction through small microchannels.[74] The flow regime is critical for avoiding aggregation and increasing dispersion.[75] In addition, synthesis in a microfluidic reactor has a greater reactive surface area and a faster mixing speed, resulting in a faster synthesis time. Microfluidic devices for the removal of fluoride ions may gain adequate adsorption interactions, a rapid adsorption rate, and precisely regulated reaction parameters, which can completely demonstrate the properties of CZFO/PPy nanocomposites with high dispersion and large specific surface area. Under the magnetic field, no nanocomposites were freed from the microfluidic device, and the fluoride solution flowed freely. The reaction strategy is illustrated in Fig. 8A. In this study, studies on fluoride adsorption were carried out utilizing a magnetically controlled microdevice. By applying a magnetic field, the magnetic CZFO/PPy nanocomposits progressively accumulated in the reaction region, and the reaction area was full with adsorbent after 2 minutes, as shown a, b, and c. The microdevice for fluoride adsorption has applications in a variety of disciplines, including water purification, and may be simply made by manipulating the magnetic field. The reaction area of magnetic CZFO/PPy nanocomposites rapidly reduced when no magnetic field was applied, and the adsorbent was washed away after 2 minutes.[50] Their work demonstrated a prototype device for continuous defluoridation of water with multiple CZFO/PPy nanocomposites synthesized in microfluidic reactors *via* microfluidic technology, which can be combined with commercially available water-purifying installations and has great potential in achieving high efficiency and cost-effective purification of water.

From the foregoing, it is evident that most polypyrrole/inorganic metallic oxide nanocomposites integrate the advantages of both polypyrrole and metallic oxide thus granting them unique hybrid thermal, physical, chemical, and mechanical properties. This advantage helps them to effectively prevent aggregation of polypyrrole, increase specific surface area, and add several active sites for adsorption. Importantly, certain adsorbents have been effectively utilized in the column approach to remove fluoride from groundwater, which has the potential for large-scale industrial use. However, the major

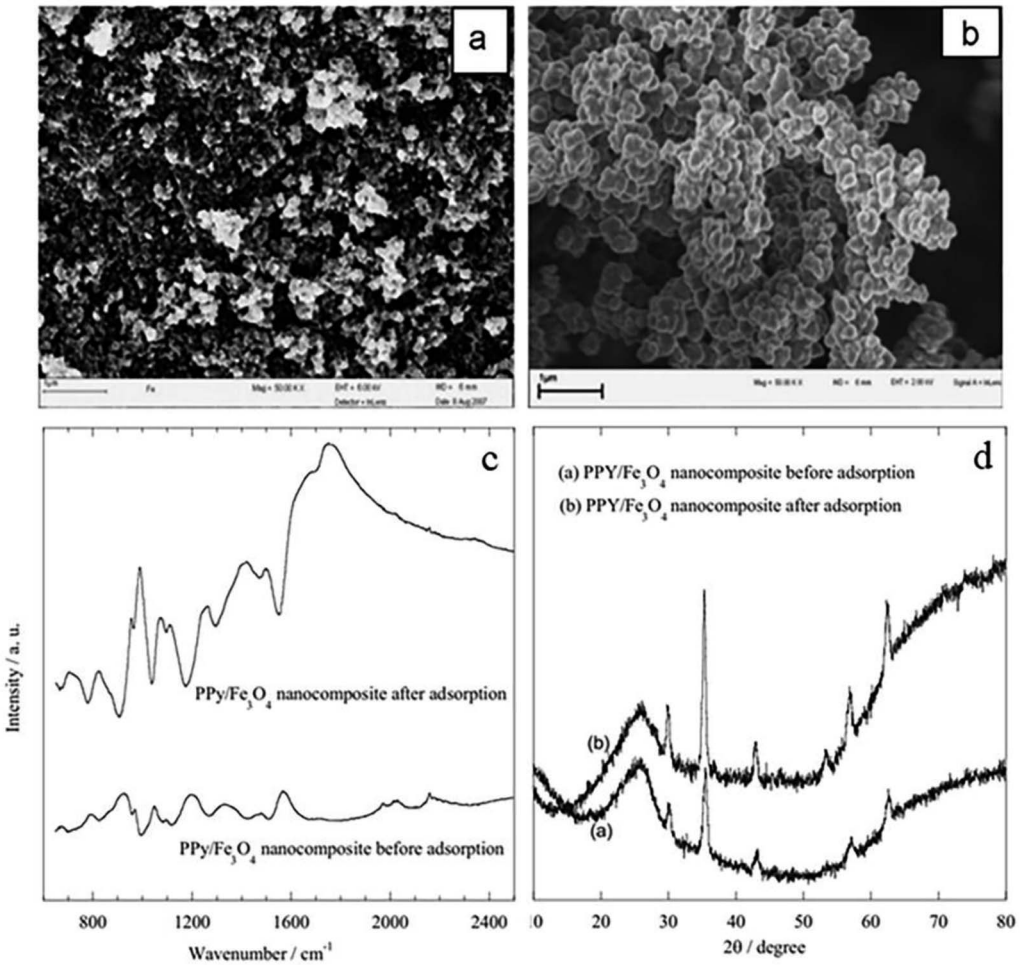

Fig. 6 FE-SEM images of (a) Fe_3O_4 nanoparticles and (b) PPy/Fe_3O_4 nanocomposite; ATR-FTIR spectra of the PPy/Fe_3O_4 nanocomposites before and after adsorption with fluoride ions (c); and XRD curve of PPy/Fe_3O_4 nanocomposite (a) before and (b) after adsorption (d).[49]

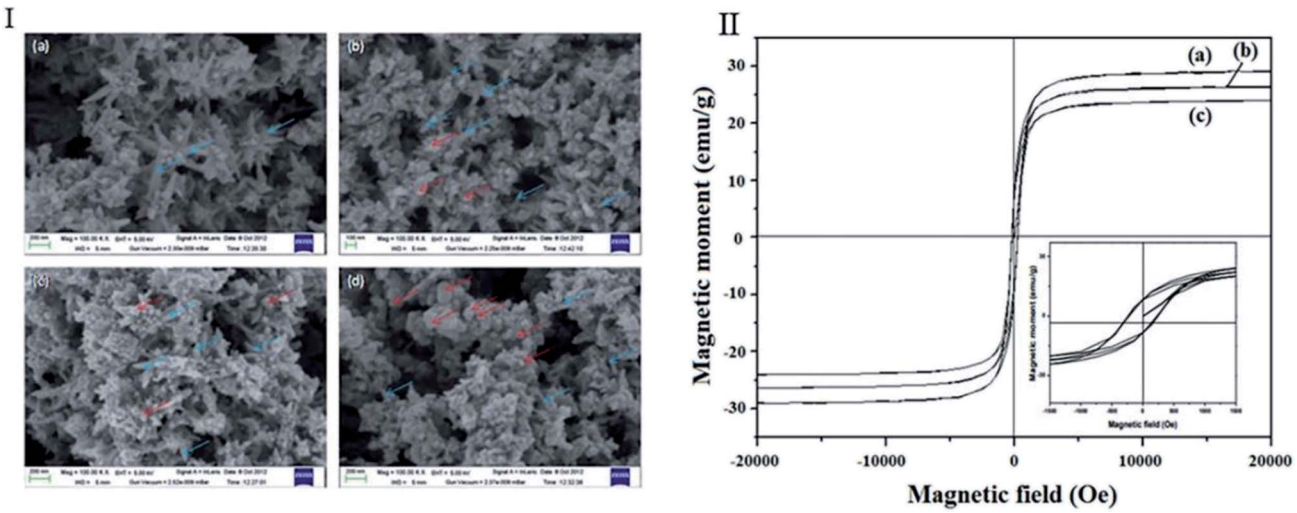

Fig. 7 FESEM image of (a) Ni nanoflower (b) Ni/PPy (2 : 1) (c) Ni/PPy (1 : 1) and (d) Ni/PPy (1 : 2) nanocomposites (I) and Room temperature magnetic property of Ni/PPy nanocomposite prepared using mass ratio of Ni : Py (a) 2 : 1, (b) 1 : 1 and (c) 1 : 2 (inset shows the corresponding magnified image of the hysteresis loop (II)).[51]

Table 3 Magnetic property of the Ni/PPy nanocomposite.[51]

No.	Ni : monomer (wt. ratio)	Saturation magnetization (emu g^{-1})	Remnant Magnetization (emu g^{-1})	Coercivity (Oe)
a	2 : 1	28.9	0.305	170
b	1 : 1	26.3	0.305	170
c	1 : 2	24.2	0.305	135

shortfall of these composites is the dissolution of metallic oxides that occurs in highly acidic solutions thus resulting in secondary pollution. Therefore, future studies should seek to increase the stability of nanocomposites to achieve uses in a wider pH range.

3. The effect of water chemistry on adsorption performance

3.1 Effect of pH

Due to the fluctuating pH values of actual wastewater, it is important to demonstrate the impact of pH on polypyrrole and polypyrrole-based adsorbents in fluoride removal. The pH of a solution affects the surface properties of polypyrrole and polypyrrole-based composites substantially. It also has a significant effect on the structural forms of fluoride ions such as HF, HF_2^-, and F^- thereby affecting its availability in the acquoes phase and bonding forms. The pH at the point of zero charges (pHpzc) helps to regulate the effect of pH on the adsorbent's surface charge. When the solution pH is less than pHpzc, the adsorbent's surface is positively charged, and when the solution pH is greater than pHpzc, the adsorbent's surface is negatively charged. The pHpzc of zero-valent $HTiO_2$@PPy, for example, was found to be 8.5.[45]. The protonation of PPy nitrogen groups and surface hydroxyl groups of $HTiO_2$ NPs caused an overall positive charge on the adsorbent's surface at an initial pH below pHpzc. Because negatively charged F^- ions react more easily with positively charged surfaces, $HTiO_2$@PPy showed superior adsorption performance on the removal of fluoride in the pH range of 3.5–8.5. The pHpzc of MgO_2/PPy nanocomposite was determined to be 5.7 by Ammavasi Nagaraj *et al.*[48] At pH 3.0, 5.0, 7.0, 9.0, and 11.0, the surface charge of MgO_2/PPy nanocomposite exhibited a positive charge in the acidic medium and negative charge in the alkaline medium, respectively. Because

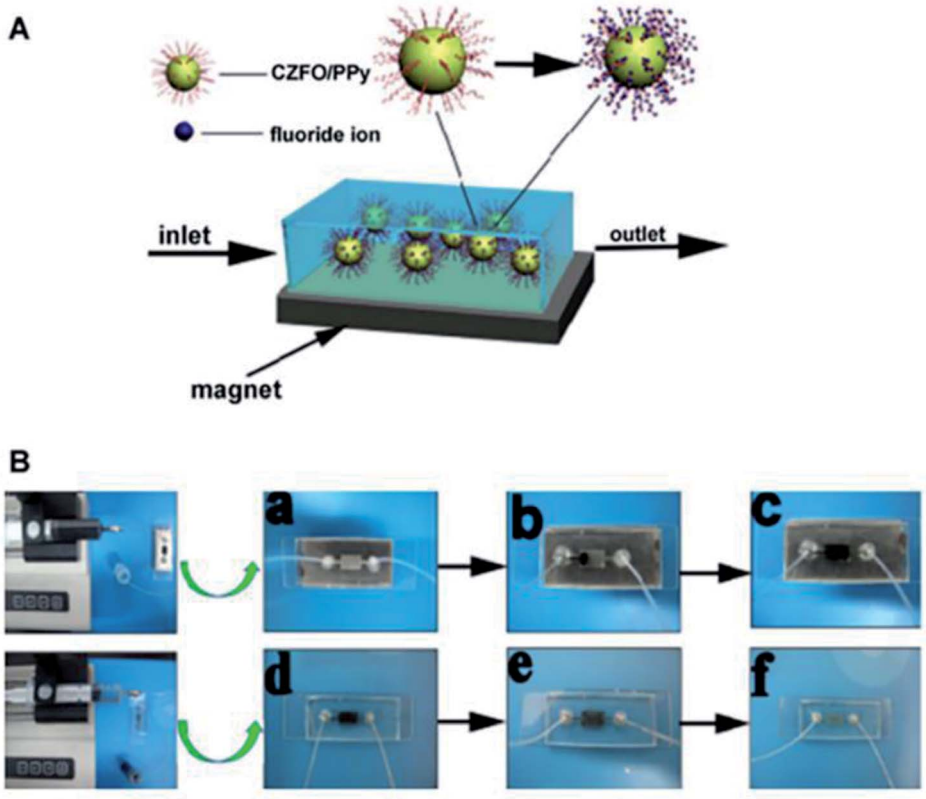

Fig. 8 Reaction scheme for fluoride adsorption in microfluidic device in magnetic field (A); photographs of the preparation and recycling process of the microfluidic device for water defluoridation (B).[50]

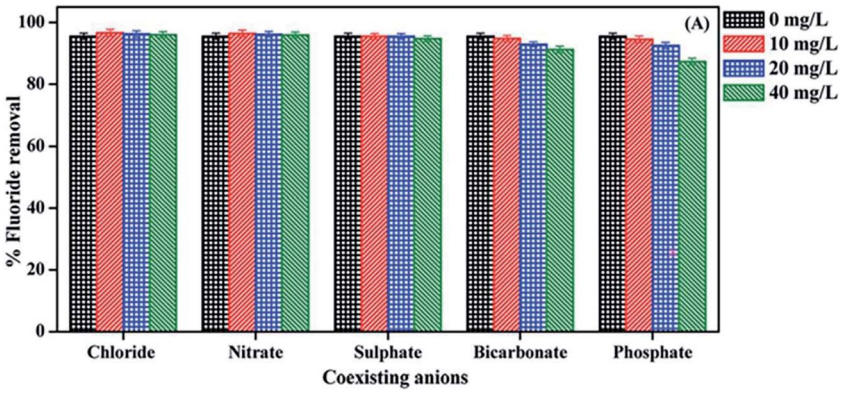

Fig. 9 Effect of coexisting anions on the F removal by $HTiO_2$@PPy.[45]

the MgO_2/PPy nanocomposite had a lower positive charge, the maximum amount of adsorption occurred only at pH 3.0, and when the pH was increased from 3.0 to 11.0, the capacity of fluoride removal decreased dramatically.

Furthermore, the initial pH of the water has a significant impact on adsorption characteristics. The protonation of the PPy nitrogen enhances the electrostatic interaction between positively charged nitrogen of the PPy and F^- ions in an aqueous solution in acidic media. Protonation of OH groups in HSnO surfaces, on the other hand, provides more positively charged active sites for F^- sorption *via* electrostatic interaction. Furthermore, F^- ions can easily exchange ions with the highly ionizable Cl^- ions that are present on the surface of PPy.[44] When pH $\geq$ pHpzc $\sim$7.6, *i.e.* under slightly alkaline conditions, coulombic repulsion begins to set in and the adsorption of fluoride start decreasing. The decrease in PPy/HSnO F^- removal efficiency can be attributed to the above two factors.[44]

3.2 Effect of water temperature

Temperature has an impact on the speeds of most reactions that increase significantly as temperatures rise. The average kinetic energy of molecules rises with temperature, according to the kinetic molecular theory, hence the migration rate of F^- ions to the active adsorption site accelerates accordingly. For example, a study reported that increasing the reaction temperature from, 298 to 328 K increased the adsorption capacity thus, demonstrating an endothermic nature of adsorption by PPy/HSnO. In addition, the equilibrium time shortens from 45 minutes to 20 minutes. This might be because greater temperatures enhance the frequency of collisions thus reaching equilibrium quickly.[44] Another investigation found that at 25 °C, the maximum adsorption capacity was 33.178 mg g^{-1}. The adsorption of F^- decreased with increasing temperature, showing that the interaction between F^- and PPy/TiO_2 was exothermic.[61]

3.3 Effect of other anions

Surface water, groundwater, and wastewater include a variety of anions that compete with fluoride for adsorbent active adsorption sites. Madhumita Bhaumik *et al.*[49] studied the effect of these co-existing anions on fluoride adsorption and discovered that both sulfate and phosphate ions can establish competitive interactions with fluoride ions, reducing adsorption marginally. This might be because fluoride, sulfate, and phosphate ions are all innersphere complex-forming species, competing for the same adsorption active sites. Wang *et al.*[35] investigated the PPy/BC nanocomposite adsorption capacity for fluoride in the presence of other anions and discovered that sulfate and bicarbonate had a significant impact on the defluoridation capacity because the carbonate and bicarbonate ions hydrolyzed in the solution, raising the pH value. As a result, the produced OH will compete with F for active adsorption sites on the adsorbent surface, reducing the number of active sites available. Furthermore, certain inorganic anions might increase coulombic repulsive forces, potentially enhancing F^- sorption. In the presence of Cl^- and NO_3^-, F^- sorption increased marginally, as seen in Fig. 9. Because Cl^- and NO_3^- are low-affinity ligands, they establish weaker interactions with active sites *via* outer-sphere complex formation and hence have less effect on F^- adsorption.[45]

4. Conclusion

This paper has reviewed relevant studies on treating fluorinated water using polypyrrole and polypyrrole-based composites. The different types of polypyrrole and polypyrrole-based composites have been summarized under four major types mainly based on their surface and structural modifications. These are (i) polypyrrole, (ii) polypyrrole bio-adsorbents, (iii) polypyrrole/clay minerals composites and (iv) polypyrrole/metallic oxide nanocomposites. The mechanism of adsorption and the influence of water chemistry parameters have been reviewed. Based on the relevant data, the following major conclusions can be drawn from this paper.

1. Polypyrrole and polypyrrole-based adsorbents are readily available adsorbents with a simple synthesis process and high environmental stability, relatively affordable with limited/no dissolution in water pollution.

2. The inclusion of different materials on polypyrrole to synthesize its composites can boost their specific surface area

ranging from 30 to 1200 m^2 g^{-1} with the advantage of enhancing adsorption capacity through exposed/available active sites.

3. Evidence also shows that modifying polypyrrole with materials such as bio-adsorbents, clay minerals composites, and metallic oxides not only increases accessible active groups but also enhances its affinity thus resulting in an increase in its pH_{PZC} which allows adsorption to occur in a wider pH range (2–12).

4. The addition of modifiers such as metal ions, and organic ligands on polyphenol also induces multiple mechanisms such as ion exchange and electrostatic attraction which occurs simultaneously thus increasing sorption effectiveness.

Therefore, utilizing polypyrrole alone to remove fluoride in the effluent is not enough since it has several limitations such as fewer adsorptive sites and restricted pH range for chemisorption.

5. Future prospects

Future studies should explore its application prospects in treating extremely acidic industrial fluoride-containing wastewater to achieve the simultaneous benefits of improved adsorption and environmental friendliness. Also, more studies should be conducted on diverse modifying agents and synthesis routes aimed at improving its stability in the aqueous phase and increasing adsorption capacity. Besides, column studies should be utilized to examine the potential of an adsorbent for large-scale applications in addition to batch studies to further implement the removal of industrial fluorinated wastewater. Desorption and regenerating studies of adsorbents should be given a priority to reduce cost and minimize the disposal of the spent adsorbent.

Conflicts of interest

The authors declare no conflict of financial interest or any others.

References

1 S. Jagtap, M. K. Yenkie, N. Labhsetwar and S. Rayalus, *Chem. Rev.*, 2012, **112**, 2454–2466.
2 Y. S. Huang, J. X. Li, X. P. Chen and X. K. Wang, *RSC Adv.*, 2014, **4**, 62160–62178.
3 S. I. Alhassan, L. Huang, Y. J. He, L. Yan, B. C. Wu and H. Y. Wang, *Crit. Rev. Environ. Sci. Technol.*, 2021, **51**, 2051–2085.
4 Y. Y. Yang, X. Du, A. Abudula, Z. L. Zhang, X. L. Ma, K. Y. Tang, X. G. Hao and G. Q. Guan, *Sep. Purif. Technol.*, 2019, **223**, 154–161.
5 C. M. Kanno, R. L. Sanders, S. M. Flynn, G. Lessard and S. C. B. Myneni, *Environ. Sci. Technol.*, 2014, **48**, 5798–5807.
6 C. L. Li, N. Chen, Y. A. Zhao, R. Li and C. P. Feng, *Chemosphere*, 2016, **163**, 81–89.
7 G. Alagumuthu and M. Rajan, *Chem. Eng. J.*, 2010, **158**, 451–457.
8 G. Zhang, Z. L. He and W. Xu, *Chem. Eng. J.*, 2012, **183**, 315–324.
9 I. J. G. f. d.-w. q. Rozov.
10 N. Azbar and A. Turkman, *Water Sci. Technol.*, 2000, **42**, 403–407.
11 H. Mjengera, G. J. P. Mkongo and C. o. t, *Earth*, 2003, **28**, 1097–1104.
12 X. H. Zhu, C. X. Yang and X. P. Yan, *Microporous Mesoporous Mater.*, 2018, **259**, 163–170.
13 W. C. Yang, S. Q. Tian, Q. Z. Tang, L. Y. Chai and H. Y. Wang, *J. Colloid Interface Sci.*, 2017, **496**, 496–504.
14 K. Y. A. Lin, Y. T. Liu and S. Y. Chen, *J. Colloid Interface Sci.*, 2016, **461**, 79–87.
15 Z. Wan, W. Chen, C. Liu, Y. Liu and C. L. Dong, *J. Colloid Interface Sci.*, 2015, **443**, 115–124.
16 H. Paudyal, B. Pangeni, K. Inoue, M. Matsueda, R. Suzuki, H. Kawakita, K. Ohto, B. K. Biswas and S. Alam, *Sep. Sci. Technol.*, 2012, **47**, 96–103.
17 L. N. Ho, T. Ishihara, S. Ueshima, H. Nishiguchi and Y. Takita, *J. Colloid Interface Sci.*, 2004, **272**, 399–403.
18 R. X. Liu, J. L. Guo and H. X. Tang, *J. Colloid Interface Sci.*, 2002, **248**, 268–274.
19 Z. Amor, B. Bariou, N. Mameri, M. Taky, S. Nicolas and A. Elmidaoui, *Desalination*, 2001, **133**, 215–223.
20 U. T. Un, A. S. Koparal and U. B. Ogutveren, *Chem. Eng. J.*, 2013, **223**, 110–115.
21 M. Thakkar, Z. Wu, L. Wei and S. J. J. C. I. Mitra, *J. Colloid Interface Sci.*, 2015, **450**, 239–245.
22 N. Mumtaz, G. Pandey and P. K. Labhasetwar, *Crit. Rev. Environ. Sci. Technol.*, 2015, **45**, 2357–2389.
23 R. Sharma, R. Sharma, K. Parveen, D. Pant and P. Malaviya, *Chemosphere*, 2021, **281**, 130892.
24 M. Vithanage and P. Bhattacharya, *Environ. Chem. Lett.*, 2015, **13**, 131–147.
25 P. Loganathan, S. Vigneswaran, J. Kandasamy and R. Naidu, *J. Hazard. Mater.*, 2013, **248**, 1–19.
26 S. S. A. Alkurdi, R. A. Al-Juboori, J. Bundschuh and I. Hamawand, *Environ. Int.*, 2019, **127**, 704–719.
27 H. N. M. E. Mahmud, A. K. O. Huq and R. B. Yahya, *RSC Adv.*, 2016, **6**, 14778–14791.
28 K. L. Wan, L. Huang, J. Yan, B. Y. Ma, X. J. Huang, Z. X. Luo, H. G. Zhang and T. F. Xiao, *Sci. Total Environ.*, 2021, **773**, 145535.
29 S. I. Alhassan, Y. J. He, L. Huang, B. C. Wu, L. J. Yan, H. Y. Deng and H. Y. Wang, *J. Environ. Chem. Eng.*, 2020, **8**, 104532.
30 L. F. Jin, L. Y. Chai, T. T. Song, W. C. Yang and H. Y. Wang, *J. Cent. S. Univ.*, 2020, **27**, 1176–1185.
31 J. Stejskal, *Chem. Pap.*, 2020, **74**, 1–54.
32 M. Karthikeyan, K. K. Satheeshkumar and K. P. Elango, *J. Hazard. Mater.*, 2009, **167**, 300–305.
33 X. Zhang and R. B. Bai, *Langmuir*, 2003, **19**, 10703–10709.
34 L. X. Xie, Z. H. Yu, S. M. Islam, K. R. Shi, Y. H. Cheng, M. W. Yuan, J. Zhao, G. B. Sun, H. F. Li, S. L. Ma and M. G. Kanatzidis, *Adv. Funct. Mater.*, 2018, **28**, 1800502.
35 J. G. Wang, N. Chen, M. Li and C. P. Feng, *J. Polym. Environ.*, 2018, **26**, 1559–1572.

36 Y. L. Xu, J. Y. Chen, R. Chen, P. L. Yu, S. Guo and X. F. Wang, *Water Res.*, 2019, **160**, 148–157.
37 M. Karthikeyan, K. K. S. Kumar and K. P. Elango, *Environ. Technol.*, 2012, **33**, 733–739.
38 E. H. Borai, M. M. E. Breky, M. S. Sayed and M. M. Abo-Aly, *J. Colloid Interface Sci.*, 2015, **450**, 17–25.
39 B. J. Pan, B. C. Pan, W. M. Zhang, L. Lv, Q. X. Zhang and S. R. Zheng, *Chem. Eng. J.*, 2009, **151**, 19–29.
40 J. T. Feng, Z. Y. Wang, W. L. Zhang, X. Y. Zhao, J. T. Zhang, Y. P. Liu and W. Yan, *Environ. Sci. Pollut. Res.*, 2021, **28**, 67267–67279.
41 M. Karthikeyan, K. K. Satheesh Kumar and K. P. Elango, *Desalination*, 2011, **267**, 49–56.
42 Y. Chen, J. Li and H. Xu, 2017.
43 M. Karthikeyan, K. K. S. Kumar and K. P. Elango, *J. Fluorine Chem.*, 2009, **130**, 894–901.
44 K. Parashar, N. Ballav, S. Debnath, K. Pillay and A. Maity, *J. Colloid Interface Sci.*, 2016, **476**, 103–118.
45 K. Parashar, N. Ballav, S. Debnath, K. Pillay and A. Maity, *RSC Adv.*, 2016, **6**, 99482–99495.
46 J. Chen, C. J. Shu, N. Wang, J. T. Feng, H. Y. Ma and W. Yan, *J. Colloid Interface Sci.*, 2017, **495**, 44–52.
47 N. Rahman and M. Nasir, *J. Water Process. Eng.*, 2017, **19**, 172–184.
48 A. Nagaraj, D. Govindaraj and M. Rajan, *Emergent Mater.*, 2018, **1**, 25–33.
49 M. Bhaumik, T. Y. Leswifi, A. Maity, V. V. Srinivasu and M. S. Onyango, *J. Hazard. Mater.*, 2011, **186**, 150–159.
50 G. Wang, G. Y. Shi, Q. H. Mu, Q. H. Zhang, H. Z. Wang and Y. G. Li, *J. Hazard. Mater.*, 2012, **237**, 1–9.
51 S. K. Srivastava, S. Senapati, S. B. Singh and P. K. Raul, *RSC Adv.*, 2016, **6**, 113424–113431.
52 S. Maity, A. Dubey and S. Chakraborty, *J. Ind. Text.*, 2021, **51**, 152–173.
53 U. Johanson, A. Marandi, T. Tamm and J. Tamm, *Electrochim. Acta*, 2005, **50**, 1523–1528.
54 E. Tchomgui-Kamga, E. Ngameni and A. Darchen, *J. Colloid Interface Sci.*, 2010, **346**, 494–499.
55 Y. A. Shang, X. Xu, B. Y. Gao and Q. Y. Yue, *J. Cleaner Prod.*, 2018, **199**, 36–46.
56 M. Chaudhary, S. Rawat, N. Jain, A. Bhatnagar and A. Maiti, *Carbohydr. Polym.*, 2019, **216**, 140–148.
57 M. Mucha, K. Wankowicz and J. Balcerzak, *e-Polym.*, 2007, **267**, 49–56.
58 R. H. Huang, L. J. Zhang, P. Hu and J. Wang, *Int. J. Biol. Macromol.*, 2016, **86**, 496–504.
59 Q. J. Du, J. K. Sun, Y. H. Li, X. X. Yang, X. H. Wang, Z. H. Wang and L. H. Xia, *Chem. Eng. J.*, 2014, **245**, 99–106.
60 V. Sivasankara, T. Ramachandramoorthy and A. Chandramohan, *J. Hazard. Mater.*, 2010, **177**, 719–729.
61 S. Chamarthy, C. W. Seo and W. E. Marshall, *J. Chem. Technol. Biotechnol.*, 2001, **76**, 593–597.
62 T. Agag and T. J. P. Takeichi, *Polymer*, 2000, **41**, 7083–7090.
63 J. W. Gilman, *Appl. Clay Sci.*, 1999, **15**, 31–49.
64 Z. Ding and R. L. Frost, *Thermochim. Acta*, 2004, **416**, 11–16.
65 Y. L. Ma, Z. R. Xu, T. Guo and P. You, *J. Colloid Interface Sci.*, 2004, **280**, 283–288.
66 A. Tor, *Desalination*, 2006, **201**, 267–276.
67 S. Q. Gu, X. N. Kang, L. Wang, E. Lichtfouse and C. Y. Wang, *Environ. Chem. Lett.*, 2019, **17**, 629–654.
68 T. T. Zhu, C. H. Zhou, F. B. Kabwe, Q. Q. Wu, C. S. Li and J. R. Zhang, *Appl. Clay Sci.*, 2019, **169**, 48–66.
69 V. B. Yadav, R. Gadi and S. Kalra, *J. Environ. Manage.*, 2019, **232**, 803–817.
70 J. H. Wang, X. J. Han, H. R. Ma, Y. F. Ji and L. J. Bi, *Chem. Eng. J.*, 2011, **173**, 171–177.
71 Y. Kong, Z. L. Wang, N. I. Jun-Hua, T. Sun and Z. D. J. J. o. I. A. Chen, 2010.
72 T. W. Luo, H. L. Xu, Z. Li, S. T. Gao, A. Ouadah, Z. Y. Zhang, Y. X. Zhang, F. Wang, C. J. Jing and C. J. Zhu, *Macromol. Mater. Eng.*, 2017, **302**, 1700095.
73 U. O. Aigbe, R. B. Onyancha, K. E. Ukhurebor and K. O. Obodo, *RSC Adv.*, 2020, **10**, 595–609.
74 M. Meier, E. M. Lucchetta and R. F. Ismagilov, *Lab Chip*, 2010, **10**, 2147–2153.
75 J. L. Steinbacher and D. T. McQuade, *J. Polym. Sci., Polym. Chem. Ed.*, 2006, **44**, 6505–6533.